

# Time-resolved tryptophan emission study of cardiac troponin I

Rongliu Liao,\* Chein-Kao Wang,<sup>†</sup> and Herbert C. Cheung<sup>‡</sup>

\*Graduate Program in Biophysical Sciences; and <sup>†</sup>Department of Biochemistry, University of Alabama at Birmingham, Birmingham, Alabama 35294-2041 USA

**ABSTRACT** We have carried out a time-resolved fluorescence study of the single tryptophanyl residue (Trp-192) of bovine cardiac TnI (CTnI). With excitation at 300 nm, the intensity decay was resolved into three components by a nonlinear least-squares analysis with lifetimes of 0.60, 2.22, and 4.75 ns. The corresponding fractional amplitudes were 0.27, 0.50, and 0.23, respectively. These decay parameters were not sensitive to complexation of CTnI with cardiac troponin C (CTnC), and magnesium and calcium had no significant effect on the decay parameters. After incubation with 3':5'-cyclic AMP-dependent protein kinase, the intensity decay of CTnI required a fourth exponential term for satisfactory fitting with lifetimes of 0.11, 0.81, 1.95, and 6.63 ns and fractional amplitudes of 0.06, 0.37, 0.27, and 0.29, respectively. When bound to CTnC, the intensity decay of phosphorylated CTnI (p-CTnI) also required four exponential terms for satisfactory fitting, but the longest lifetime increased by a factor of 1.7. The decay parameters obtained from the complex formed between p-CTnI and CTnC were not sensitive to either magnesium or calcium. The anisotropy decay was resolved into two components with rotational correlation times of 0.90 and 23.48 ns. Phosphorylation resulted in a decrease of the long correlation time to 14.61 ns. The anisotropy values recovered at zero time suggest that the side chain of the Trp-192 had considerable subnanosecond motional freedom not resolved in these experiments. Within the CTnI · CTnC complex, the unresolved fast motions appeared sensitive to calcium binding to the calcium-specific site of CTnC. The observed emission heterogeneity is discussed in terms of possible excited-state interactions in conjunction with the predicted secondary structure of CTnI. The loss of molecular asymmetry of cardiac troponin I induced by phosphorylation as demonstrated in this work may be related to the known physiological effect of  $\beta$ -agonists on cardiac contractility.

## INTRODUCTION

A key step in the activation of vertebrate striated muscle is binding of activator calcium to the three-subunit troponin bound to the actin filament. The transfer of this calcium signal from its receptor protein troponin C (TnC) to distal actin sites involves tropomyosin and the other two subunits of troponin, troponin I (TnI), and troponin T (TnT) (Hitchcock et al., 1973; Margossian and Cohen, 1973; Potter and Gergely, 1974). In skeletal muscle, fluorescence resonance energy transfer studies have suggested that the initial events resulting from the binding of activator calcium to TnC may include global intrasubunit and intersubunit movements of specific regions of TnC and TnI (Wang and Cheung, 1986; Tao et al., 1989) and alterations of conformational fluctuations in these proteins (Lakowicz et al., 1988; Cheung et al., 1991). Energetic studies have also indicated that the interaction between TnC and TnI plays a dominant role in signal transmission (Wang and Cheung, 1985). Thus, TnI may serve as the major molecular transmitter of the calcium signal in activation of skeletal muscle (Cheung et al., 1987; Tao et al., 1990). While less structural and energetic information is available for cardiac muscle, the free energy coupling for the interaction of cardiac TnC (CTnC) with cardiac TnI (CTnI) and calcium also suggests the importance of the troponin I subunit in signal transduction in this muscle (Liao et al., 1989).

Skeletal TnC has four sites for calcium. Two sites (sites I and II) are located in the NH<sub>2</sub>-terminal half of the mole-

cule and bind calcium specifically with a low affinity, and the other two sites located in the COOH-terminal half bind calcium with a high affinity and also bind magnesium competitively. Since the low affinity sites are calcium-specific, they play a major regulatory role in calcium regulation. Both skeletal TnC and CTnC have similar molecular weights. When compared with the sequence of skeletal TnC (Collins et al., 1977), the 12-residue binding loop of site I in cardiac TnC has several amino acid substitutions (Van Eerd and Takahashi, 1976) and is unable to chelate calcium, thus leaving site II as the only site in CTnC for binding activator calcium. Skeletal TnI from rabbit muscle has 178 amino acids, and bovine cardiac TnI has 211 amino acids. The main difference between these two proteins is an additional 33 amino acids (residues 1–33) at the amino-terminus of CTnI (Leszyk et al., 1988). The amino-terminal extension of residues is also present in cardiac TnI, but not in skeletal TnI, from other species. This stretch of the polypeptide has several residues that can be readily phosphorylated, including a serine that can be phosphorylated *in vitro* by cAMP-dependent protein kinase (Stull and Buss, 1977). The same residue is also phosphorylated in perfused heart during  $\beta$ -stimulation (Solaro et al., 1976). We (Cheung and Liao, 1990) have recently shown that the phosphorylation of CTnI decreases its affinity for CTnC by a factor of  $\sim 3$  regardless of whether the low affinity site of TnC is occupied by calcium, and the lost affinity is recovered upon dephosphorylation of the phosphorylated protein. Detailed balance requires that the affinity of the complex formed between phosphorylated CTnI and CTnC for Ca<sup>2+</sup> decreased by a similar factor when compared with nonphosphorylated com-

Address correspondence to H. C. Cheung.

R. Liao's present address is Division of Cardiology, Beth Israel Hospital, Boston, MA 02215.

C.-K. Wang's present address is Department of Physiology and Biophysics, University of Washington, Seattle, WA 98195.

plex. An early study showed a small rightward shift of the pCa (to higher  $\text{Ca}^{2+}$  concentration) vs. fluorescence curve for labeled CTnC in cardiac troponin reconstituted with phosphorylated CTnI (Robertson et al., 1982), compatible with the recent binding results.

In the absence of high resolution spectroscopic data on the structures of any of the cardiac troponin subunits, it is not yet possible to understand the mechanistic detail of signal transduction in cardiac muscle at the residue level. However, the single tryptophanyl residue in position 192 of CTnI provides a signal for probing localized conformations of the protein. In this paper, we report on the time-resolved fluorescence of the Trp-192 in cardiac troponin I and the effect of phosphorylation of the protein on the dynamics of the fluorescence properties.

## MATERIALS AND METHODS

### Protein preparation

Cardiac troponin was extracted from an ether powder that was prepared from the left ventricles of fresh bovine hearts (Potter, 1982). The troponin subunits were separated and initially isolated from one another on a CM-Sephadex C-50-120 column in the presence of 6 M urea, 50 mM Tris, pH 8.0, 1 mM EDTA, and 0.1 mM DTT. Crude CTnC was eluted without a gradient, and the other two subunits were eluted with a NaCl gradient from 0 to 0.6 M. The isolated crude CTnI was rechromatographed on a DEAE-Sephadex A-50 column in 6 M urea, 20 mM imidazole, pH 7.0, 1 mM EDTA, and 0.1 mM DTT, and eluted without salt. Crude CTnC was purified by a separate DEAE-Sephadex A-50 column under identical conditions and eluted with a gradient from 0 to 0.1 M KCl. The purity of the two proteins was monitored by NaDodSO<sub>4</sub> polyacrylamide gel electrophoresis. The purified proteins were lyophilized in the presence of 0.1 M KCl, 0.5 mM EGTA, 0.5 mM DTT, 20 mM imidazole, pH 7.2, and stored at  $-20^{\circ}\text{C}$ .

CTnI was phosphorylated essentially as described by Perry and Cole (1974) by incubation of the protein (typically 1–2 mg/ml) with bovine cardiac 3':5'-cyclic AMP-dependent protein kinase (0.01 mg/ml) in a buffer containing 50 mM Tris, pH 7.2, 50 mM  $\alpha$ -glycerophosphate, 5 mM  $\text{MgCl}_2$ , 25 mM NaF, 1 mM DTT, 0.1 mM cAMP. The reaction was started by addition of ATP to a final concentration of 1 mM, and the mixture was incubated at  $30^{\circ}\text{C}$  for 5 min, followed by dialysis against a buffer containing 50 mM Tris, pH 7.2, 0.4 M KCl, 1 mM EGTA, and 15 mM  $\beta$ -mercaptoethanol at pH 7.5. The dialyzed protein was applied to a Sephadex G-100 superfine column ( $2.6 \times 100$  cm) equilibrated with the dialysis buffer. The eluted phosphorylated CTnI (p-CTnI) was used for fluorescence studies.

Control CTnI was prepared in parallel experiments without addition of ATP. For reaction with radioactive ATP, [ $\gamma$ - $^{32}\text{P}$ ]ATP was used. Bound  $^{32}\text{P}$  was quantitated by scanning autoradiograms of 12% NaDodSO<sub>4</sub> polyacrylamide slab gels with a laser densitometer. This procedure typically incorporated 1.7–1.8 mol of P/mol CTnI. Samples treated with nonradioactive ATP were used for physical measurements. The binary complex CTnT · CTnC was prepared by incubating CTnI with a 1.5-fold stoichiometric excess of CTnC. Under this condition, better than 99% of CTnI or phosphorylated CTnI was complexed with CTnC (Cheung and Liao, 1990).

### Steady-state fluorescence measurements

Steady-state emission spectra were recorded on a Perkin-Elmer MPF-66 spectrofluorometer (Norwalk, CT) linked to a PE 7200 computer. Quantum yields of troponin I were determined by the comparative method (Parker and Reese, 1960) using L-tryptophan as the standard.

A value of 0.14 was used as the quantum yield of the amino acid (Valeur and Weber, 1977). Steady-state quenching of tryptophanyl fluorescence was performed by addition of 6 M acrylamide with excitation at 295 nm, and the emission was monitored at the peak of the unquenched spectrum. A correction was made for inner filter effect arising from absorbance of acrylamide.

### Time-correlated fluorescence measurements

Initial intensity decay measurements of the tryptophanyl residue were made on an instrument equipped with a 5-W Spectra Physics 171-09 argon ion laser (San Jose, CA) that was mode-locked to generate pulses at a repetition rate of 82 MHz. These pulses were used to excite a Rhodamine 6G dye in ethylene glycol in a jet stream dye laser. A cavity dumper was used to reduce the output pulse rate to 800 kHz. The red output from the cavity dumper was frequency-doubled to 295 nm with an angle-tuned KDP crystal and was used as the excitation light. The detection system was a time-correlated single photon-counting system equipped with a Hamamatsu R955 PM tube (Bridgewater, NJ). The excitation pulses generated by this system were typically in the range of 600–700 ps in half-width.

Anisotropy decays and additional intensity decays were measured with 300 nm excitation on an instrument located at the University of Oregon (Ruggiero and Hudson, 1989). This system used a mode-locked Spectra Physics CW Nd:YAG solid state laser as the pumping source for the dye laser and a Hamamatsu R1294U electrostatically focused microchannel plate photomultiplier tube operated at 3,200 V as the detector. The half-width of the instrument response profile was  $\sim 70$  ps. The emitted light was detected at 360 nm through a 10-nm band-pass Corion interference filter (Holliston, MA). The time base was 20 ps/channel in a total of 1,024 channels. All measurements of CTnI samples were made at  $20^{\circ}\text{C}$  in a medium containing 0.4 M KCl, 25 mM MOPS, pH 7.2, 1 mM DTT, and 1 mM EGTA. When  $\text{Ca}^{2+}$  was present,  $\text{CaCl}_2$  was added to a final concentration of 1.5 mM; when  $\text{Mg}^{2+}$  was present,  $\text{MgCl}_2$  was added to 3 mM.

A nonlinear least-squares iterative reconvolution procedure was used to recover intensity decay parameters by fitting the data to a sum of exponential terms (Marquardt, 1963; Grinvald and Steinberg, 1974):

$$F(t) = \sum_i \alpha_i \exp(-t/\tau_i). \quad (1)$$

The analysis program included optimization of stray light and a time shift between the instrument response function and observed data. The goodness of a fit between observed data and the chosen function was evaluated by the following statistics: the reduced chi-square ratio ( $\chi^2_R$ ), the weighted residuals, the autocorrelation function of the residuals, the runs test (Gunst and Mason, 1980), and the Durbin-Watson parameter (D-W). The D-W examines the correlation between the residual values in neighboring channels (Lampert et al., 1983). The following D-W values are considered adequate for the number of exponential terms ( $i$ ) in the model: for  $i = 1$ ,  $\text{D-W} > 1.7$ ;  $i = 2$ ,  $\text{D-W} > 1.75$ ;  $i = 3$ ,  $\text{D-W} > 1.8$ . The log-likelihood ratio test (Gross and Clark, 1975) was also used to further discriminate between two decay models. The same procedure was used to fit the anisotropy decay data with a biexponential function,

$$r(t) = r_0 \sum_{i=2} g_i \exp(-t/\phi_i), \quad (2)$$

where the total anisotropy recovered at zero time is given by  $r_0 = r_0 g_1 + r_0 g_2$ , and  $\sum g_i = 1.0$ .

TABLE 1 Relative quantum yield of Trp-192 in cardiac troponin I\*

Sample	Rel. $Q$	$K_{sv}$	Sample	Rel. $Q$	$K_{sv}$
		$M^{-1}$			$M^{-1}$
CTnI	1.00	12.8	p-CTnI	1.13	10.1
CTnI · CTnC	1.14	12.9	p-CTnI · CTnC	1.31	10.8
CTnI · CTnC + $Mg^{2+}$	1.14	12.9	p-CTnI · CTnC + $Mg^{2+}$	1.31	10.8
CTnI · CTnC + $Ca^{2+}$	1.21	11.3	p-CTnI · CTnC + $Ca^{2+}$	1.34	12.9

\* The quantum yield of nonphosphorylated troponin I (CTnI) was 0.086 and that of phosphorylated troponin I (p-CTnI) was 0.097. The relative quantum yield (Rel.  $Q$ ) of various samples is given relative to the quantum yield of nonphosphorylated CTnI. CTnI · CTnC is the complex formed between CTnI and CTnC, and p-CTnI · CTnC is the complex formed between phosphorylated CTnI and CTnC.  $K_{sv}$  is the Stern-Volmer constant for acrylamide quenching obtained from the initial slope of a plot of  $F_0/F$  vs. acrylamide concentration, where  $F_0$  is the intensity in the absence of acrylamide, and  $F$  the intensity in the presence of acrylamide.

## RESULTS

### Steady-state fluorescence of CTnI and phosphorylated CTnI

The steady-state emission spectrum of CTnI showed a peak at 346 nm (data not shown). The emission peak remained essentially unchanged upon phosphorylation. Complexation of CTnI with CTnC resulted in a blue shift of 6 to 340 nm, whereas complexation of p-CTnI with CTnC resulted in a blue shift to 342 nm. The quantum yield of CTnI was 0.086 and that of phosphorylated CTnI was 0.097. These and other steady-state spectral parameters given in Table 1.

The solvent accessibility of the Trp-192 was determined using acrylamide as the fluorescence quencher. The Stern-Volmer plots in every case displayed a downward curvature beyond  $\sim 150$  mM (data not shown). Also given in Table 1 are the Stern-Volmer constant ( $K_{sv}$ ) determined from the initial slopes of the plots for both nonphosphorylated and phosphorylated CTnI and their complexes with CTnC.

### Intensity decay of CTnI

The intensity decay of the Trp-192 of CTnI was complex. Every set of decay data was analyzed by a sum of exponential terms, and in each case the data clearly could not be satisfactorily fitted to either a monoexponential or a biexponential function. Fig. 1 shows a typical intensity decay curve with 300-nm excitation. The fit was significantly improved with the triexponential function. The recovered three lifetimes were well separated: 0.60, 2.22, and 4.75 ns, with each component making a significant contribution to the total emission (Table 2). To further discriminate between the biexponential and triexponential fits, we used the log-likelihood ratio test to show that the three-exponential fit was justified over the two-exponential fit. Also listed in Table 2 are the decay parameters recovered from the complex CTnI · CTnC in the presence of different ligands. In each case the lifetime values were also well separated and each had a significant contribution to the total fluorescence.

### Anisotropy decay of CTnI

A representative anisotropy decay curve of CTnI is shown in Fig. 2. The data were adequately fitted with a biexponential function, yielding two rotational correlation times ( $\phi_1 = 0.90$  ns and  $\phi_2 = 23.48$  ns). The long component contributed 35% to the total recovered zero-time anisotropy  $r_0$ . These and other results obtained under different conditions are listed in Table 3. When bound to CTnC, the long correlation time  $\phi_2$  increased to 30.28 ns, whereas the change in  $\phi_1$  was negligible. The contribution of  $\phi_2$  to the total anisotropy decreased somewhat to 30%, but this decrease was recovered in the presence of  $Mg^{2+}$ , an ionic condition similar to that in relaxed muscle. Addition of  $Ca^{2+}$  to replace bound  $Mg^{2+}$  at the two high affinity sites III and IV and concomitantly saturate the regulatory site II reduced the contribution of  $\phi_2$  down to 27%. The long correlation time of the complex increased by 4 ns in the presence of  $Mg^{2+}$  and remained relatively unchanged when  $Mg^{2+}$  was replaced by  $Ca^{2+}$ . In every case, the recovered total anisotropy was substantially lower than that expected of free tryptophan excited at 300 nm.

### Intensity decay of phosphorylated CTnI

The intensity decay of the Trp-192 of phosphorylated CTnI is very different from that of nonphosphorylated CTnI. Fig. 3 shows that the decay data could not be fitted to a triexponential function. Four exponential terms were required to yield a satisfactory fit with lifetimes in the range of 0.11–6.63 ns. The log-likelihood ratio test indicated that the four-exponential model was justified over the three-exponential model. These data for p-CTnI and those recovered for the complex formed between p-CTnI and CTnC are given in Table 4. As in the case of nonphosphorylated CTnI, the recovered lifetime values were well separated with the ratio of any two lifetimes always larger than 2. This decay pattern provides an assurance that the analysis of the complex decay is reasonable. In spite of the presence of a fourth decay component, the weighted mean lifetime of p-CTnI was 3.13 ns as compared with 3.26 ns for nonphosphorylated CTnI.

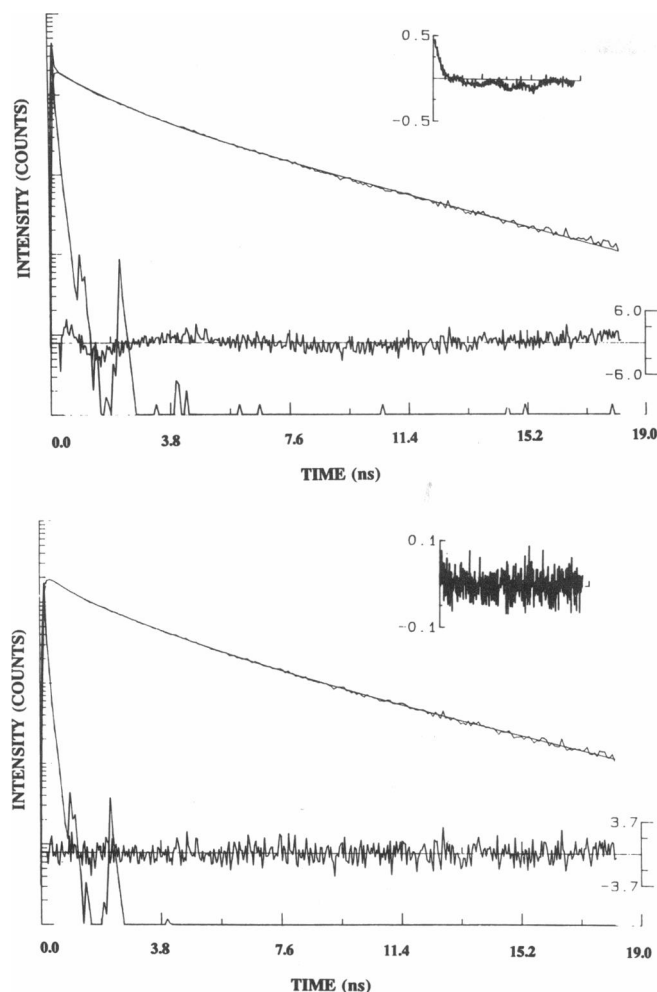


FIGURE 1 Fluorescence intensity decay of Trp-192 of bovine cardiac troponin I ( $\sim 5 \times 10^{-5}$  M).  $\lambda_{\text{ex}} = 300$  nm, and  $\lambda_{\text{em}} = 360$  nm. The narrow and sharp peak shown on the left of the figure is the instrument response profile. The lower tracing across the figure is the weighted residual plot, and the inset at the upper right-hand corner is the autocorrelation function of the residuals. (Upper) The data were fitted to a biexponential function, with  $\chi^2_{\text{R}} = 1.64$ , D-W = 1.24, and  $Z_{\text{run}}$  (runs test) = 8.22. (Lower) The data were fitted to a triexponential function, with  $\chi^2_{\text{R}} = 0.98$ , D-W = 2.03, and  $Z_{\text{run}}$  (runs test) = 1.24. The best fitted parameters are listed in Table 2. The triexponential fit is much improved over the biexponential fit with acceptable fitting statistics. The log-likelihood ratio test was also used to demonstrate that the triexponential fit was justified over the other fit. Other experimental conditions are given in the text.

The decay of p-CTnI · CTnC differed from that of uncomplexed p-CTnI in three ways. Firstly, the longest lifetime  $\tau_4$  increased from 6.63 to 11.07 ns. Secondly, the fractional amplitude associated with the shortest lifetime increased from 0.06 to 0.34 at the expense of the longest lifetime:  $\alpha_4$  decreasing from 0.29 to 0.07. Thirdly, the weighted mean lifetime increased by  $\sim 3$  to 6.15 ns. A substantial perturbation of the Trp-192 environment in CTnI was induced by complexation with troponin C. However, the decay parameters of the protein complex were not sensitive to the addition of either  $\text{Mg}^{2+}$  or  $\text{Ca}^{2+}$ .

## Anisotropy decay of phosphorylated CTnI

Phosphorylation of CTnI produced substantial changes in the anisotropy decay of the protein. Given in Table 5 are the anisotropy decay parameters for uncomplexed p-CTnI and the complex p-CTnI · CTnC in the presence of  $\text{Mg}^{2+}$  and  $\text{Ca}^{2+}$ . Two rotational correlation times were still resolved from the decay curve of p-CTnI, but  $\phi_1$  was reduced from 0.90 to 0.29 ns and  $\phi_2$  from 23.48 to 14.61 ns. The fractional contribution of the long component now increased from 0.34 to 0.44. If  $\phi_2$  is taken to reflect the overall motion of the protein, the 38% decrease suggests that p-CTnI could be considerably more compact than CTnI. The recovered total anisotropy was higher than for nonphosphorylated protein, but still less than the expected value for free tryptophan. In the phosphorylated complex p-CTnI · CTnC,  $\phi_1$  was not affected and  $\phi_2$  increased by a factor of 1.35 to 19.79 ns as compared with uncomplexed p-CTnI. This increase, which reflects the larger mass of the binary protein complex, is comparable to that for the nonphosphorylated system. In the presence of  $\text{Mg}^{2+}$  and  $\text{Ca}^{2+}$ ,  $\phi_2$  increased in a manner similar to nonphosphorylated CTnI · CTnC.

## DISCUSSION

The steady-state emission spectrum of the Trp-192 of cardiac troponin I suggests the residue to be in a relatively polar environment. This environment becomes less polar when the protein is bound to CTnC, as reflected by a blue shift of the emission peak and a 14% increase in quantum yield. In the binary complex CTnI · CTnC, the quantum yield is not affected by the presence of magnesium. However, a small increase is observed when magnesium in the solution is replaced by calcium. Phosphorylation does not affect the emission maximum of CTnI, but increases the quantum by 13%. When bound to CTnC, the steady-state emission properties of p-CTnI change in a manner similar to those of nonphosphorylated CTnI: a 4-nm blue shift and a 16% increase in quantum yield. Similarly, the quantum yield is unaffected by the presence of magnesium, but slightly increased in the presence of calcium. Although the increase in quantum yield is small, the results suggest that calcium binding to the single calcium-specific site in CTnC is sensed by the single Trp in CTnI bound to CTnC. A consequence of this  $\text{Ca}^{2+}$  binding is a shift of the Trp-192 to a slightly less polar environment, and this localized conformational change appears independent of the state of phosphorylation of TnI.

The downward curvature observed in the Stern-Volmer plots suggests the presence of multiple decay components for the single Trp residue. The Stern-Volmer constants indicate that the residue is highly quenched and hence highly accessible to solvent collisions. This accessibility is reduced upon phosphorylation as the  $K_{\text{sv}}$  is reduced by 22%. Since the dynamic

TABLE 2 Intensity decays of Trp-192 in cardiac troponin I and its complex with cardiac troponin C\*

Sample	Condition	$\tau_i$	$\alpha_i$	$f_i$	$\langle\tau\rangle$	$\chi_R^2$	D-W
		ns			ns		
CTnI	EGTA	0.60 (3) 2.22 (7) 4.75 (8)	0.27 (1) 0.50 (1) 0.23 (2)	0.07 0.47 0.46	3.26	0.98	2.03
CTnI · CTnC	EGTA	0.57 (3) 2.20 (6) 4.80 (8)	0.27 (1) 0.51 (1) 0.22 (1)	0.07 0.49 0.45	3.26	1.06	2.02
CTnI · CTnC	Magnesium	0.52 (3) 2.10 (5) 4.62 (7)	0.27 (1) 0.50 (1) 0.23 (1)	0.06 0.46 0.48	3.21	1.11	2.03
CTnI · CTnC	Calcium	0.67 (3) 2.37 (7) 5.03 (3)	0.29 (1) 0.54 (1) 0.17 (2)	0.08 0.55 0.37	3.22	0.98	1.88

\* CTnI  $\approx 50 \mu\text{M}$ . The complex CTnI · CTnC was obtained by incubating CTnI with a 1.5-fold stoichiometric excess of CTnC for several hours before measurement. See text for other conditions. Excitation wavelength was 300 nm. The standard deviations obtained from the least-squares fitting are given in parentheses in units of 0.01 ns for the lifetimes  $\tau_i$  and 0.01 for the fractional amplitudes  $\alpha_i$ . The weighted mean lifetime was obtained from  $\langle\tau\rangle = \sum \alpha_i \tau_i^2 / \sum \alpha_i \tau_i$ , and the fractional intensity from  $f_i = \alpha_i \tau_i / \sum \alpha_i \tau_i$ .

quenching constant  $k_q$  is related to  $K_{SV}$  by  $k_q = K_{SV}/\langle\tau\rangle$ ,  $k_q$  is  $3.9 \times 10^9 \text{ M}^{-1} \text{ s}^{-1}$  for CTnI and  $3.2 \times 10^9 \text{ M}^{-1} \text{ s}^{-1}$  for p-CTnI. The former value is near the value ( $4 \times 10^9 \text{ M}^{-1} \text{ s}^{-1}$ ) for acrylamide quenching of tryptophan in proteins with a fully exposed residue (Eftink and Ghiron, 1976). This residue becomes less exposed after the protein is phosphorylated.  $\text{Mg}^{2+}$  does not affect the accessibility of the residue in CTnI · CTnC or p-CTnI · CTnC. However,  $\text{Ca}^{2+}$  binding to CTnC has different effects on the accessibility of the Trp 192 in the two complexes: it protects the residue from quenching in the nonphosphorylated complex and enhances the quenching in the phosphorylated complex. The inter-subunit structural relationship of the  $\text{Ca}^{2+}$ -specific site of CTnC with CTnI is

modified by phosphorylation of CTnI. This is an indication of the modulation effect of phosphorylation on the transfer of the signal of activator calcium from CTnC to CTnI.

The three-component intensity decay is compatible with the steady-state acrylamide quenching results and similar to our previous reports of a triexponential decay of the single Trp of rabbit skeletal TnI from time-domain (Wang et al., 1985) and frequency-domain (Lakowicz et al., 1988) measurements. This finding of multiple exponential decay is consistent with the decay properties of many single-tryptophan proteins (Ludescher et al., 1985; Vincent et al., 1988; Chabbert et al., 1991).

The anisotropy decay of CTnI is resolved into two components. The short component is  $\sim 1$  ns regardless of whether the protein is unbound or bound to CTnC. About 65–72% of the recovered total anisotropy decays with the 1-ns component. This short correlation time may be attributed to either the motion of the indole ring or an internal motion of a segment of the polypeptide in which Trp-192 is located. The long correlation time of 23.48 ns can be attributed to the overall motion of the protein itself. An equivalent spherical rigid rotor with a hydration of 0.3 g of water/g of protein has a rotational correlation time of 10 ns, considerably smaller than the observed value. If CTnI is approximated by a prolate ellipsoid of revolution, its two rotational correlation times can be readily calculated using appropriate frictional coefficients (Koeing, 1975) and a value of  $0.73 \text{ ml} \cdot \text{g}^{-1}$  as the partial specific volume (Byers and Kay, 1983) for different assumed values of hydration and axial ratio. For an axial ratio of 5, the harmonic means of the two calculated correlation times are 22, 25, and 27 ns if the hydration value is assumed to be 0.2, 0.3, and 0.4, respectively. Assuming that the observed long correlation time can be approximated by the harmonic mean of the two correlation times of an ellipsoid of revolution,

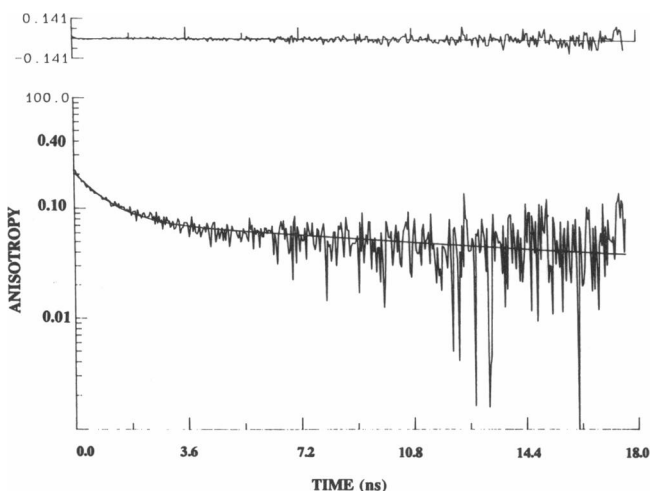


FIGURE 2 A representative plot for the anisotropy decay of the Trp-192 of bovine cardiac troponin I.  $\lambda_{ex} = 300 \text{ nm}$ ,  $\lambda_{em} = 360 \text{ nm}$ . The data were fitted to a biexponential function, yielding two rotational correlation times:  $\phi_1 = 0.90 \text{ ns}$ ,  $\phi_2 = 23.48 \text{ ns}$ ,  $\chi_R^2 = 1.05$ , and D-W = 2.04. Other conditions were the same as for Fig. 1.

TABLE 3 Anisotropy decays of Trp-192 in cardiac troponin I and its complex with cardiac troponin C\*

Sample	Condition	$\phi_i$	$g_i r_0$	$r_0$	$\theta$ (deg)	$\chi_R^2$	D-W
		ns					
CTnI	EGTA	0.90 (2)	0.145 (10)	0.222	46.0	1.05	2.04
		23.48 (10)	0.077 (3)				
CTnI · CTnC	EGTA	1.15 (1)	0.143 (10)	0.205	42.9	1.05	1.98
		30.28 (6)	0.062 (1)				
CTnI · CTnC	Magnesium	1.11 (1)	0.145 (10)	0.228	45.0	1.08	1.97
		34.40 (13)	0.083 (1)				
CTnI · CTnC	Calcium	1.21 (1)	0.146 (2)	0.200	50.6	1.10	1.74
		36.06 (7)	0.054 (1)				

\* The conditions are the same as for Table 2. The anisotropy decay was resolved into two components, with  $\phi_1$  referring to the rotational correlation time of the short component and  $\phi_2$  to the correlation time of the long component. The total anisotropy is given by  $r_0 = g_1 r_0 + g_2 r_0$ , where  $g_1$  and  $g_2$  are the amplitudes of the short and long components, respectively.  $\theta$  is the angular range corresponding to the rotational mode of the short correlation time. The numbers given in parentheses are the standard deviations from the least-squares fitting in units of 0.01 ns for the correlation times and 0.001 for the amplitudes.

these and similar calculations show that the observed long correlation time of CTnI is compatible with an axial ratio of 4–5 with hydration in the range of 0.2–0.4. Hydrodynamic studies (Byers and Kay, 1983) have shown that CTnI is not a compact globular protein, in agreement with the present anisotropy results. The complex CTnI · CTnC is also asymmetric, and this asymmetry may be somewhat enhanced when CTnC is saturated with magnesium. The overall shape of the complex appears to be affected by cation binding to one of the two constituent proteins and this shape change is sensed by the tryptophanyl residue in the other protein.

Phosphorylation of CTnI results in a decrease in both correlation times. We have suggested that the long correlation time arises from the overall motion of the protein. This single correlation time, however, does not in itself indicate isotropic rotation and is probably an average of the correlation times of anisotropic rotation. An obvious cause for the decrease of the long correlation time is loss of molecular asymmetry of the protein. A fourth intensity decay component appears with a lifetime of 6.63 ns for phosphorylated CTnI. This value is within the range of multiple lifetimes for four-component decays which have been reported for single-tryptophan proteins (Ludescher et al., 1985; Vincent et al., 1988). Our four-component fit of the intensity decay is statistically acceptable, but the three-component fit is not. We are confident of this analysis. That the local conformation of Trp 192 is different in phosphorylated CTnI is supported by the quantum yield and acrylamide quenching results. The three shortest lifetimes recovered for phosphorylated CTnI are shorter than the three lifetimes for non-phosphorylated protein. Since short lifetimes may bias detection of anisotropy decay toward short correlation times, the smaller correlation times observed with phosphorylated protein could, in part, be accounted for by this redistribution of the decay components. A third possibility is that phosphorylation alters the average orientations of transition dipoles with respect to the principal

rotational diffusion axis of the protein. The relationship of these orientations to the diffusion coefficients and hence the correlation times is complex (Harvey and Cheung, 1977; Small and Isenberg, 1977; Barkley et al., 1981). It is difficult to assess this possibility from present experimental data, but any change in the structure surrounding the residue side chain is likely coupled to changes in the relative orientations. The change in dipole orientations would have to be very drastic to bring about the observed large decrease in the long correlation time. Because of the uncertainties of the various factors, we believe that the simplest interpretation of the decreased correlation time is a decrease of the axial ratio of the protein. If hydration is not much affected by phosphorylation, a value of 15 ns for the harmonic mean of the two correlation times is compatible with an axial ratio of  $\sim 2$  as compared with a ratio of 4–5 for nonphosphorylated CTnI.

Upon complexation with CTnC, the intensity decay of Trp 192 of p-CTnI also shows four components, but the longest lifetime is now  $\sim 11$  ns with a dominant contribution to the total intensity. Such a long lifetime for tryptophan in proteins is unusual, but not unprecedented (Ludescher et al., 1985; Casas-Finet et al., 1990). The origin of the long lived decay component is unclear. The steady-state and quenching data are consistent with the lifetime data, indicating an altered environment for Trp 192. As expected, the long correlation time of p-CTnI · CTnC (19.79 ns) is smaller than that of CTnI · CTnC (30.28 ns). This fractional decrease (0.65) is comparable to that observed between uncomplexed p-CTnI and CTnI (0.62). The increase of the long correlation time from uncomplexed CTnI to CTnI · CTnC is also comparable to the increase from p-CTnI to p-CTnI · CTnC. Thus, the phosphorylation-induced loss in the asymmetry of CTnI is carried over to its complex with CTnC.

The apparent total anisotropy values recovered from the anisotropy decay curves are in the range of 0.20–

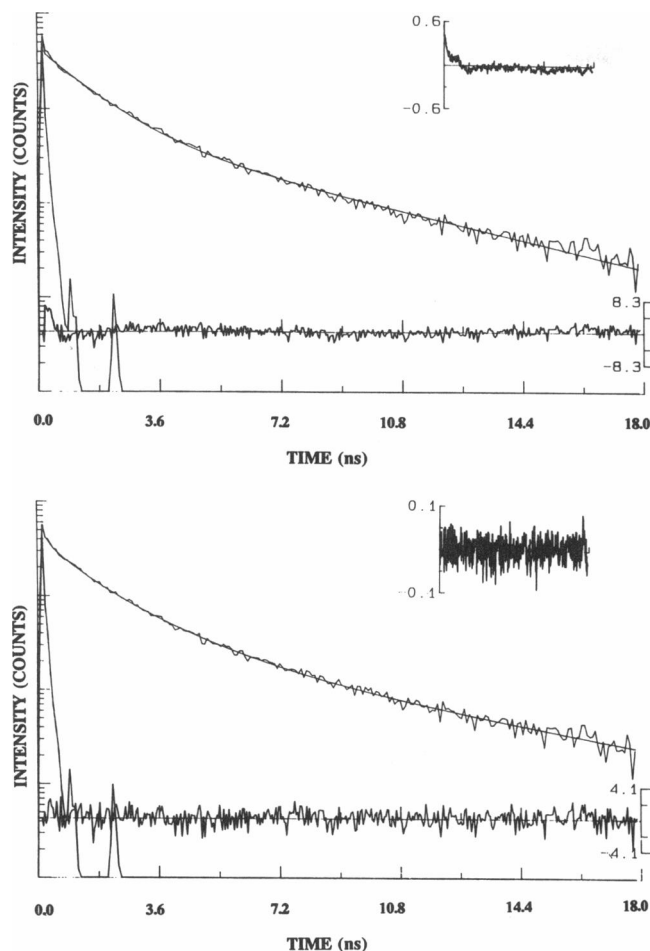


FIGURE 3 Fluorescence intensity decay of the Trp-192 of phosphorylated cardiac troponin I from bovine muscle. (Upper) The data were fitted to a triexponential function, with  $\chi^2_R = 1.34$ , D-W = 1.19, and  $Z_{\text{run}} = -6.63$ . (Lower) The data were fitted to a sum of four exponential terms, with  $\chi^2_R = 1.09$ , D-W = 1.86, and  $Z_{\text{run}} = -1.22$ . These two fits were subjected to the log-likelihood ratio test, and the result showed that the four-exponential fit was justified over the other fit. Conditions were the same as for Fig. 1.

0.26, considerably smaller than the value of 0.31 expected for free tryptophan when excited at 300 nm (Valeur and Weber, 1977). The smaller values indicate the presence of some subnanosecond motions that were not recovered in these experiments. Since the instrument used for the anisotropy decay experiments had a time resolution down to 70 ps, the undetected fast motions are likely below 100 ps. There is a further loss in  $r_0$  when CTnI is bound to CTnC, which indicates the presence of additional fast motions resulting from interaction between the two proteins. This loss is recovered upon addition of magnesium. When magnesium is replaced by calcium, the apparent anisotropy is reduced from 0.228 to 0.200. Calcium binding to the specific site of CTnC enhances the motional freedom of the Trp-192 of CTnI in the protein complex. The amplitude of the motion of the residue is larger in calcium than in magnesium, as indi-

cated by the larger angular range ( $\theta$ ) of the rotational mode corresponding to this motion in the presence of calcium. A similar calcium-induced enhancement of the freedom of the residue also occurs with phosphorylated CTnI.

The amino acid sequences of TnI from five different muscles are known, including bovine and rabbit cardiac muscles and rabbit and avian skeletal muscles. Each of these sequences contains a single Trp residue located in the middle of an invariant heptapeptide sequence (Val-Gly-Asp-Trp-Arg-Lys-Asn) (Leszyk et al., 1988). This feature suggests that the single Trp may play a functional role. While this report does not address the latter question, it is important to examine some of the molecular processes that can account for the observed Trp-192 emission heterogeneity. In the absence of crystallographic information or other types of high resolution spectroscopic data, it is useful to examine the secondary structure of CTnI by using both the CF (Chou and Fasman, 1978) and the GOR (Garnier et al., 1978) methods. The CF method predicts 9  $\alpha$ -helical segments totalling 72%  $\alpha$ -helix and a single  $\beta$ -sheet structure. The GOR method predicts 68%  $\alpha$ -helicity distributed among 5  $\alpha$ -helical segments, and 3 regions of  $\beta$ -sheet structure accounting for  $\sim 7\%$  of the protein. Both methods predict several long helices: a 39-residue segment at residues 151–189 by CF and a 44-residue segment at residues 30–73 by GOR. These predictions are summarized in Fig. 4. The first 29 residues at the amino-terminus have no  $\alpha$ -helicity, but includes the first  $\beta$ -sheet predicted by GOR. This segment represents most of the amino-terminal extension of the polypeptide of CTnI not found in skeletal TnI. The third  $\beta$ -sheet structure predicted by GOR at residues 145–150 coincides with the single  $\beta$ -sheet structure predicted by CF at residues 144–150. A comparison of the  $\beta$ -turn regions predicted by both methods suggest 5  $\beta$ -turns at residues 3–7, 25–28, 77–80, 137–140, and 199–203. The first 4 turns are based on predictions by both methods, whereas the last turn is based only on the CF method.

The single Trp at position 192 is predicted to be located in a short segment that is neither an  $\alpha$ -helix nor a  $\beta$ -sheet, and also predicted to have a surface probability of 11.7 (Emini et al., 1985). These structural features would allow the tryptophan side chain considerable motional freedom and are compatible with the steady-state spectral parameters, the Stern-Volmer constant for acrylamide quenching, and anisotropy results. There are potential transient interactions between the excited-state of the indole ring and neighboring residues that can affect the nonradiative decay rate of the indole ring. These neighboring residues include Asp-191, Asp-197, and Ser-200, which is at the amino end of the helical segment at the COOH-terminus. Carboxyl groups can destabilize the excited-state of the indole ring and result in emission with higher energies (Szabo and Rayner, 1980). If such an interaction occurs, the short lifetimes would be fa-

TABLE 4 Intensity decays of Trp-192 in phosphorylated cardiac troponin I and its complex with cardiac troponin C\*

Sample	Condition	$\tau_i$	$\alpha_i$	$f_i$	$\langle\tau\rangle$	$\chi_R$	D-W
		<i>ns</i>			<i>ns</i>		
p-CTnI	EGTA	0.11 (1) 0.81 (2) 1.95 (1) 6.63 (3)	0.06 (3) 0.37 (4) 0.27 (10) 0.29 (10)	0.02 0.16 0.52 0.30	3.13	1.09	1.86
p-CTnI · CTnC	EGTA	0.11 (0.1) 0.70 (3) 2.37 (1) 11.07 (4)	0.34 (3) 0.31 (10) 0.27 (10) 0.07 (3)	0.02 0.13 0.38 0.47	6.15	1.02	2.13
p-CTnI · CTnC	Magnesium	0.13 (0.1) 0.67 (0.1) 2.22 (0.4) 11.61 (2)	0.28 (0.3) 0.31 (10) 0.34 (10) 0.08 (1)	0.02 0.11 0.40 0.47	6.46	0.98	1.92
p-CTnI · CTnC	Calcium	0.12 (0.4) 0.71 (0.4) 2.15 (1) 11.69 (3)	0.28 (1) 0.32 (2) 0.34 (1) 0.06 (2)	0.02 0.13 0.42 0.43	6.00	0.98	1.94

\* The conditions are the same as for Table 2. The numbers given in parentheses are the standard deviations from the least-squares fitting in units of 0.01 ns for the lifetimes and 0.01 for the fractional amplitudes.

vored at the blue edge of the emission spectrum. The present data are insufficient for this analysis. Since hydroxyls can form exciplexes with indole derivatives, an interaction of a serine residue with the Trp could alter its nonradiative decay rate. These interactions are unlikely static and can be expected to fluctuate in time, dependent upon the rate with which the indole ring can move and the rate of dynamic fluctuation of localized structure. Since the anisotropy decay results indicate that the Trp side chain can move on the subnanosecond time regime, the putative interactions are expected to change during the excited-state lifetime and can give rise to the observed multiple exponential decay of CTnI. The appearance of a fourth decay component with phosphorylated CTnI could result from alteration of these excited-state interactions of the indole ring. Whatever the mechanism leading to multiple decay times, we could estimate the radiative ( $k_r$ ) and nonradiative ( $k_{nr}$ ) decay rates of Trp-192 from the expressions  $k_r = Q/(\sum \alpha_i \tau_i)$  and  $k_{nr} = k_r/Q - k_r$  (Werner and Foster, 1979), where  $Q$  is the

quantum yield. The values of  $k_r$  and  $k_{nr}$  are  $0.036 \times 10^9 \text{ s}^{-1}$  and  $0.38 \times 10^9 \text{ s}^{-1}$ , respectively. When compared with the  $k_r$  ( $0.050 \times 10^9 \text{ s}^{-1}$ ) and  $k_{nr}$  ( $0.31 \times 10^9 \text{ s}^{-1}$ ) for *N*-acetyl-L-tryptophanamide (NATA), the radiative rate of Trp-192 of CTnI is 30% smaller and the nonradiative rate is 22% larger. The observed smaller quantum yield of CTnI in comparison with NATA is thus due to a combination of both effects. Similar calculations suggest that, in the complex CTnI · CTnC,  $k_r$  increases slightly and  $k_{nr}$  is not affected when  $\text{Mg}^{2+}$  is replaced by  $\text{Ca}^{2+}$ . The small increase in the quantum yield of the Trp-192 in CTnI · CTnC in response to activator  $\text{Ca}^{2+}$  binding results from a slightly more favorable radiative decay rate. While phosphorylation does not affect the radiative rate, it appears to reduce the nonradiative rate. This reduction can account for the 13% increase in quantum yield resulting from phosphorylation. For p-CTnI · CTnC, the radiative rates in the absence and presence of  $\text{Mg}^{2+}$  or  $\text{Ca}^{2+}$  are either comparable to or slightly higher than that for NATA, but the corresponding nonradiative

TABLE 5 Anisotropy decays of Trp-192 in phosphorylated cardiac troponin I and its complex with cardiac troponin C\*

Sample	Condition	$\phi_i$	$g_i r_0$	$r_0$	$\theta$ (deg)	$\chi_R^2$	D-W
		<i>ns</i>					
CTnI	EGTA	0.29 (1) 14.61 (7)	0.148 (10) 0.110 (10)	0.248	45.0	1.12	2.03
CTnI · CTnC	EGTA	0.31 (1) 19.79 (14)	0.146 (4) 0.118 (10)	0.264	40.6	1.13	2.00
CTnI · CTnC	Magnesium	0.17 (1) 21.13 (14)	0.180 (10) 0.082 (2)	0.262	47.9	1.08	2.30
CTnI · CTnC	Calcium	0.30 (1) 23.64 (23)	0.124 (1) 0.071 (4)	0.195	45.0	1.06	1.97

\* All conditions are the same as for Table 3. The numbers given in parentheses are the standard deviations from the least-squares fitting in units of 0.01 ns for the correlation times and 0.001 for the amplitudes.



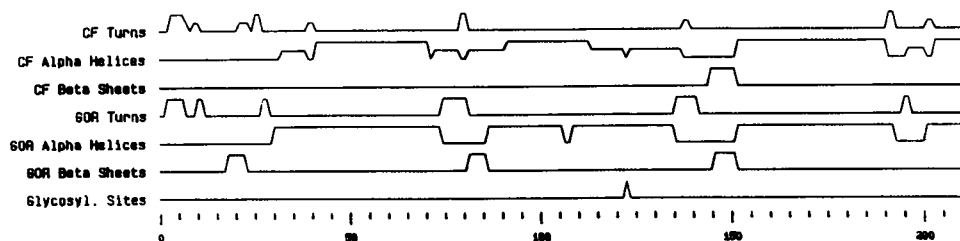


FIGURE 4 Secondary structure prediction of cardiac troponin I. CF, prediction by Chou and Fasman (1978); and GOR, prediction by Garnier, Osguthorpe, and Robson (1978). The predictions were made with the UWGCG (University of Wisconsin Genetics Computer Group) software package. In this package, the original CF rules are slightly modified as follows: helix, the conditions that  $p(\text{bound}) > 1.0$  and that  $p(\alpha) > p(\beta)$  are not used; sheet, a minimum length of five residues is required. The original GOR method is also slightly modified: the minimum length of a helix is changed to six and that of a  $\beta$ -sheet is four. Regions that cannot be adequately predicted are replaced by the conformational state of the next best probability.

rates are also larger. The differences in  $k_r$  and  $k_{nr}$  between nonphosphorylated and phosphorylated CTnI·CTnC complexes clearly indicate different environments for the Trp-192 in the two forms of CTnI in the protein complex.

The phosphorylation of CTnI results in a large change in the hydrodynamic shape of the protein. An early study indicated that, with incubation conditions similar to those used in this present work, cAMP-dependent protein kinase readily phosphorylated Ser-20 and more slowly Ser-146 of rabbit cardiac TnI (Moir and Perry, 1977). These two residues correspond to Ser-23 and Ser-151 in bovine cardiac TnI (Leszyk et al., 1988). Ser-23 may be important because it is conserved in cardiac TnI, whereas Ser-151 is an invariant in all known sequences of TnI from both cardiac and skeletal muscles (Leszyk et al., 1988). Thus, the residues phosphorylated in our sample could be Ser-23 and Ser-151. A more recent study indicated that both Ser-23 and Ser-24 of bovine cardiac TnI were phosphorylated in troponin by cAMP-dependent protein kinase (Swiderek et al., 1988). At this time, the sites that were phosphorylated with our incubation conditions are not resolved. In spite of this uncertainty, the phosphorylation induces significant conformational changes. To what extent the observed decrease in correlation time may be attributed to phosphorylation of Ser 23 (and Ser 24) or Ser 151 is not resolved in this work. If the effect is due predominantly to phosphorylation of sites in the  $\text{NH}_2$ -terminal extension, the known relaxation effect of  $\beta$ -agonists on cardiac contractility could be related to an increase in the molecular symmetry of CTnI.

We thank Dr. Bruce Hudson for the use of his picosecond fluorometer and Dr. Ian Johnson for valuable assistance and discussion during the course of the picosecond measurements.

This work was supported, in part, by a Graduate Fellowship from the University of Alabama at Birmingham (awarded to R. Liao) and by NIH grant AR25193 (to H. Cheung).

Received for publication 15 November 1991 and in final form 11 May 1992.

## REFERENCES

- Barkley, M. D., A. J. Kowalczyk, and L. Brand. 1981. Fluorescence decay studies of anisotropic rotations of small molecules. *J. Chem. Phys.* 75:3581-3593.
- Byers, D. M., and C. M. Kay. 1983. Hydrodynamic properties of bovine cardiac troponin C. *J. Biol. Chem.* 258:2951-2954.
- Casas-Finet, J. R., R. L. Karpel, and S. H. Wilson. 1990. Biophysical studies on the mammalian heterogeneous nuclear ribonucleoprotein, A1, and its component domains. *SPIE 1204 (Time-Resolved Laser Spectroscopy in Biochemistry II)*: 540-547.
- Chabbert, M., T. L. Lukas, D. M. Watterson, P. H. Axelsen, and F. G. Prendergast. 1991. Fluorescence analysis of calmodulin mutants containing tryptophan: conformational changes induced by calmodulin-binding peptides from myosin light chain kinase and protein kinase II. *Biochemistry*. 30:7615-7630.
- Cheung, H. C., and R. Liao. 1990. Effect of phosphorylation of cardiac troponin I on its interaction with cardiac troponin C. The 10th International Biophysics Congress, Vancouver, Canada. p. 125.
- Cheung, H. C., C.-K. Wang, and N. A. Malik. 1987. Interaction of troponin subunits: free energy of binary and ternary complexes. *Biochemistry*. 26:5904-5907.
- Chou, P. Y., and G. D. Fasman. 1978. Empirical predictions of protein conformation. *Annu. Rev. Biochem.* 47:251-276.
- Cheung, H. C., C.-K. Wang, I. Gryczynski, W. Wiczek, G. Laczko, M. L. Johnson, and J. R. Lakowicz. 1991. Distance distribution and anisotropy decays of troponin C and its complexes with troponin I. *Biochemistry*. 30:5238-5247.
- Collins, J. H., M. L. Greaser, J. D. Potter, and M. J. Horn. 1977. Determination of the amino acid sequence of troponin C from rabbit skeletal muscle. *J. Biol. Chem.* 252:6356-6362.
- Cross, A. J., and G. R. Fleming. 1984. Analysis of time-resolved fluorescence anisotropy decays. *Biophys. J.* 46:45-56.
- Emeni, E. A., J. V. Hughes, D. S. Perlow, and J. Boger. 1985. Induction of hepatitis A virus-neutralizing antibody by a virus-specific synthetic peptide. *J. Virol.* 55:836-839.
- Eftink, M. R., and C. A. Ghiron. 1976. Exposure of tryptophanyl residues in proteins. Quantitative determination by fluorescence quenching studies. *Biochemistry*. 15:672-680.
- Garnier, J., D. J. Osguthorpe, and B. Robson. 1978. Analysis of the accuracy and implications of simple methods for predicting the secondary structure of globular proteins. *J. Mol. Biol.* 120:97-120.
- Grinvald, A., and I. Z. Steinberg. On the analysis of fluorescence decay kinetics by the method of least-squares. *Anal. Biochem.* 59:583-589.
- Gross, A. J., and V. A. Clark. 1975. *Survival Distributions: Reliability Application in the Biomedical Sciences*. John Wiley and Sons, New York. 228-233.

- Gunst, R. F., and R. L. Mason. 1980. In *Regression Analysis and Its Application*. Marcel Dekker, New York. 231–241.
- Harvey, S. C., and H. C. Cheung. 1977. Fluorescence depolarization studies on the flexibility of myosin rod. *Biochemistry*. 16:5181–5187.
- Hitchcock, S. E., H. Huxley, and A. G. Szent-Gyorgyi. 1973. Calcium sensitive binding of troponin to actin-tropomyosin: a two-site model for troponin action. *J. Mol. Biol.* 80:825–836.
- Johnson, J. D., J. H. Collins, S. P. Robertson, and J. D. Potter. 1980. A fluorescent probe study of  $\text{Ca}^{2+}$  binding to the  $\text{Ca}^{2+}$ -specific sites of troponin and troponin C. *J. Biol. Chem.* 255:9635–9640.
- Koeing, S. 1975. Brownian motion of an ellipsoid. A correction to Perrin's results. *Biopolymers*. 14:2421–2423.
- Lakowicz, J. R., I. Gryczynski, H. C. Cheung, C.-K. Wang, M. L. Johnson, and N. Joshi. 1988. Distance distribution in proteins recovered by using frequency-domain fluorometry: applications to troponin I and its complexes with troponin C. *Biochemistry*. 27:9149–9160.
- Lampert, R. A., L. A. Chewter, D. Phillips, D. V. O'Connor, A. J. Roberts, and S. R. Meech. 1983. Standards for nanosecond fluorescence decay time measurements. *Anal. Chem.* 55:68–73.
- Leszyk, J., R. Dumaswala, J. D. Potter, and J. H. Collins. 1988. Amino acid sequences of bovine cardiac troponin I. *Biochemistry*. 27:2821–2827.
- Liao, R., C.-K. Wang, and H. C. Cheung. 1989. Fluorescence studies of the interaction of troponin C and troponin I from bovine cardiac muscle. *Biophys. J.* 55:273a. (Abstr.)
- Ludescher, R. D., J. J. Volwerk, G. H. de Haas, and B. S. Hudson. 1985. Complex photophysics of the single tryptophan of porcine pancreatic phospholipase  $\text{A}_2$ , its zymogen, and an enzyme/micelle complex. *Biochemistry*. 24:7240–7249.
- Margossian, S. S., and C. Cohen. 1973. Troponin subunit interactions. *J. Mol. Biol.* 81:409–413.
- Marquardt, D. W. 1963. An algorithm for least-squares estimation of nonlinear parameters. *J. Soc. Ind. Appl. Math.* 11:431–441.
- Moir, A. J. G., and S. V. Perry. 1977. The sites of phosphorylation of rabbit cardiac troponin I by adenosine 3':5'-cyclic monophosphate-dependent protein kinase. *Biochem. J.* 167:333–343.
- Parker, C. A., and W. T. Reese. 1960. Correction of fluorescence spectra and measurement of fluorescence quantum efficiency. *Analyst*. 85:587–600.
- Perry, S. V., and H. A. Cole. 1974. Phosphorylation of troponin and the effects of interaction between the components of the complex. *Biochem. J.* 141:733–743.
- Potter, J. D., and J. Gergely. 1974. Troponin, tropomyosin, and actin interactions in the  $\text{Ca}^{2+}$  regulation of muscle contraction. *Biochemistry*. 13:2697–2703.
- Potter, J. D. 1982. Preparation of troponin and its subunits. *Methods Enzymol.* 85:241–263.
- Robertson, S. P., J. D. Johnson, M. J. Holroydes, E. G. Kranias, J. D. Potter, and R. J. Solaro. 1982. The effect of troponin I phosphorylation on the  $\text{Ca}^{2+}$ -binding properties of the  $\text{Ca}^{2+}$  regulatory site of bovine cardiac troponin. *J. Biol. Chem.* 257:260–263.
- Ruggiero, A., and B. Hudson. 1989. Critical density fluctuations in lipid bilayers detected by lifetime heterogeneity. *Biophys. J.* 55:1111–1124.
- Small, E. W., and I. Eisenberg. 1977. Hydrodynamic properties of a rigid molecule: rotational and linear diffusion and fluorescence anisotropy. *Biopolymers*. 16:1907–1928.
- Solaro, R. J., A. G. J. Moir, and S. V. Perry. 1976. Phosphorylation of troponin I and the inotropic effect of adrenaline in the perfused rabbit heart. *Nature (Lond.)*. 262:615–617.
- Stull, J. T., and J. E. Buss. 1977. Phosphorylation of cardiac troponin by cyclic adenosine 3':5'-monophosphate-dependent protein kinase. *J. Biol. Chem.* 252:851–857.
- Swiderek, K., J. Kornelia, H. E. Myer, and L. M. G. Heilmeyers Jr. 1988. Cardiac troponin I, isolated from bovine heart, contains two adjacent phosphoserines. A first example of phosphoserine determination by derivatization to S-ethylcysteine. *Eur. J. Biochem.* 176:335–342.
- Szabo, A. G., and D. M. Rayner. 1980. Fluorescence decay of tryptophan conformers in aqueous solution. *J. Am. Chem. Soc.* 102:554–563.
- Tao, T., E. Gowell, G. M. Strasburg, J. Gergely, and P. C. Leavis. 1989.  $\text{Ca}^{2+}$  dependence of the distance between Cys-98 of troponin C and Cys-133 of troponin I in the ternary troponin complex. Resonance energy transfer measurements. *Biochemistry*. 28:5902–5908.
- Tao, T., B.-J. Gong, and P. C. Leavis. 1990. Calcium-induced movement of troponin-I relative to actin in skeletal muscle thin filaments. *Science (Wash. DC)*. 247:1339–1341.
- Valeur, B., and G. Weber. 1977. Resolution of the fluorescence excitation spectrum of indole into its  $^1\text{L}_a$ - $^1\text{L}_b$  excitation bands. *Photochem. Photobiol.* 25:441–444.
- Van Eerd, J. P., and K. Takahashi. 1976. Determination of the complete amino acid sequence of bovine cardiac troponin C. *Biochemistry*. 15:1171–1180.
- Vincent, M., J.-C. Brochon, F. Merola, W. Jordi, and J. Gallay. 1988. Nanosecond dynamics of horse heart apocytochrome c in aqueous solution as studied by time-resolved fluorescence of the single tryptophan residue (Trp-59). *Biochemistry*. 27:8752–8761.
- Wang, C.-K., I. Johnson, T. Ruggiero, D. Harris, and H. C. Cheung. 1985. Time-resolved fluorescence anisotropy decay of the tryptophan of skeletal troponin I and its complex with troponin C. *Biophys. J.* 47:472a. (Abstr.)
- Wang, C.-K., and H. C. Cheung. 1986. Proximity relationship in the binary complexes formed between troponin I and troponin C. *J. Mol. Biol.* 191:509–521.
- Werner, T. C., and L. S. Foster. 1979. The fluorescence of tryptophanyl peptides. *Photochem. Photobiol.* 29:905–914.